

# Dynamic Localization of RNase MRP RNA in the Nucleolus Observed by Fluorescent RNA Cytochemistry in Living Cells

Marty R. Jacobson, Long-Guang Cao, Yu-Li Wang, and Thoru Pederson

Cell Biology Group, Worcester Foundation for Biomedical Research, Shrewsbury, Massachusetts 01545

**Abstract.** The dynamic intra-nuclear localization of MRP RNA, the RNA component of the ribonucleoprotein enzyme RNase MRP, was examined in living cells by the method of fluorescent RNA cytochemistry (Wang, J., L.-G. Cao, Y.-L. Wang, and T. Pederson. 1991. *Proc. Natl. Acad. Sci. USA.* 88:7391–7395). MRP RNA very rapidly accumulated in nucleoli after nuclear microinjection of normal rat kidney (NRK) epithelial cells. Localization was specifically in the dense fibrillar component of the nucleolus, as revealed by immunocytochemistry with a monoclonal antibody against fibril-

larin, a known dense fibrillar component protein, as well as by digital optical sectioning microscopy and 3-D stereo reconstruction. When MRP RNA was injected into the cytoplasm it was not imported into the nucleus. Nuclear microinjection of mutant MRP RNAs revealed that nucleolar localization requires a sequence element (nucleotides 23–62) previously implicated as a binding site for a nucleolar protein, the To antigen. These results demonstrate the dynamic localization of MRP RNA in the nucleus and provide important insights into the nucleolar targeting of MRP RNA.

**R**IBONUCLEASE MRP<sup>1</sup> (for mitochondrial RNA processing) was initially identified as an endoribonuclease that produces, *in vitro*, RNA primers for the initiation of mitochondrial DNA replication (Chang and Clayton, 1987a). When RNase MRP was subsequently discovered to be a ribonucleoprotein enzyme and its RNA (MRP RNA; see Fig. 1) component was sequenced (Chang and Clayton, 1987b), it turned out to be identical to a previously defined nucleolar RNA, termed 7-2 RNA (Reddy et al., 1981; Gold et al., 1989; Yuan et al., 1989). MRP RNA (7-2 RNA) is essential for RNase MRP enzymatic activity *in vitro* and is encoded by a nuclear gene (Chang and Clayton, 1987b; Yuan et al., 1989; Tooper and Clayton, 1990) that is transcribed by RNA polymerase III (Chang and Clayton, 1989). MRP RNA has been detected by *in situ* hybridization in both mitochondria and nucleoli of mouse cardiac myocytes (Li et al., 1994). The great majority of MRP RNA (7-2 RNA) in the cell fractionates with nucleoli (Reddy et al., 1981).

Genetic studies in yeast have demonstrated a role for both the RNA and a protein component of RNase MRP in the 5'-end cleavage of the 5.8 S–25 S rRNA intermediate

(Schmitt and Clayton, 1993; Chu et al., 1994; Lygerou et al., 1994). In HeLa cells, nuclear MRP RNA is associated with large nucleolar structures sedimenting at ~80 S (Kiss et al., 1992). MRP RNA-containing RNP particles can be immunoprecipitated by human To (Reddy et al., 1983), Th (Hashimoto and Steitz, 1983), and Wa (Reimer et al., 1988) sera (To, Th, and Wa representing patient codes for autoimmune sera that contain antibodies directed against the MRP RNA-containing RNP particle). The protein recognized by anti-To and anti-Wa antibodies is a ~40,000-mol wt nucleolar protein (Reimer et al., 1988). The 40,000-mol wt To autoantigen-binding domain was subsequently localized to nucleotides 21–64 of human MRP RNA (Yuan et al., 1991).

In the present investigation, we have examined the subcellular localization of fluorescently tagged MRP RNA after microinjection into the nucleus of living cells. This method, which we term fluorescent RNA cytochemistry, is integrated with high resolution optical microscopy and digital image processing, and provides dynamic information while also identifying nuclear sites of high affinity for the introduced RNA. Our results show that MRP RNA is rapidly accumulated in the dense fibrillar component of the nucleolus after nuclear microinjection. In addition, we demonstrate that the To antigen-binding site is necessary for nucleolar localization of MRP RNA. These results identify the MRP RNA To antigen-binding site as a nucleolar targeting domain and provide new insights into the process of MRP RNA nucleolar localization.

Address all correspondence to T. Pederson, Cell Biology Group, Worcester Foundation for Biomedical Research, 222 Maple Avenue, Shrewsbury, MA 01545. Tel.: (508) 842-8921. Fax: (508) 842-7762.

1. *Abbreviations used in this paper:* DFC, dense fibrillar component; MRP, mitochondrial RNA processing; NRK, normal rat kidney.

## Materials and Methods

### Plasmids, In Vitro Transcription, and Fluorescent Labeling of RNA

The methods used in this study were essentially as described previously (Wang et al., 1991) with only minor modifications. Human MRP RNA was transcribed from EcoRI digested plasmid pHMRP<sub>MODT3</sub> (kindly provided by T. Kiss and W. Filipowicz, Friedrich Miescher-Institut) using T3 RNA polymerase (GIBCO-BRL, Gaithersburg, MD). Plasmids encoding mutant MRP RNAs were constructed by either deletion (pHMRP<sub>MODT3</sub>-1) or inversion (pHMRP<sub>MODT3</sub>-2) of the 40 base-pair AvrII fragment (nucleotides 23-62) of the parental plasmid pHMRP<sub>MODT3</sub>. MRP-1 and MRP-2 RNAs were transcribed from EcoRI digested plasmids pHMRP<sub>MODT3</sub>-1 and pHMRP<sub>MODT3</sub>-2, respectively, using T3 RNA polymerase.

All RNAs were transcribed from their appropriately digested plasmid DNAs in the presence of 1 mM ATP, CTP, GTP, UTP (Pharmacia LKB Biotechnology, Piscataway, NJ), and 0.1 mM 5-(3-aminoallyl)-UTP (Sigma Chem. Co., St. Louis, MO) by T3 RNA polymerase under the conditions described by the supplier. When desired, 2  $\mu$ M [ $\alpha$ -<sup>32</sup>P]CTP (New England Nuclear Research Products, Boston, MA) was added to the transcription reaction as a tracer. The RNA was recovered by ethanol precipitation and coupled either to tetramethylrhodamine-5-isothiocyanate (TRITC, isomer G; Molecular Probes, Eugene, OR) or fluorescein-5-isothiocyanate (FITC; Molecular Probes) as previously described (Langer et al., 1981; Agrawal et al., 1986; Wang et al., 1991). After coupling, the fluorochrome-labeled RNA was purified by gel filtration on a 5-ml Bio-Gel P-60 (BioRad, Hercules, CA) column. RNA from the peak column fractions was twice ethanol precipitated, and then resuspended in sterile 5 mM Tris-acetate buffer (pH 7.0) at a concentration of  $\sim$ 50  $\mu$ g/ml and centrifuged in a 42.2Ti rotor at 25,000 rpm for 30 min to remove any residual precipitate which might complicate microinjection (Beckman Instrs., Fullerton, CA). The integrity of the fluorescently labeled RNA was examined by agarose gel electrophoresis. All RNAs were heat denatured at 75°C and rapidly cooled to room temperature just before microinjection.

### RNP Assembly and Immunoprecipitation

In vitro transcribed MRP RNA was incubated for 30 min at 30°C followed by an additional 30 min at 0°C in a 50- $\mu$ l reaction containing 50% (vol/vol) HeLa cell S100 fraction (Patton et al., 1987), 1 mM ATP, 20  $\mu$ g yeast tRNA, 75 mM KCl, 2.2 mM MgCl<sub>2</sub>, 0.25 mM dithiothreitol, and 20 mM Hepes (pH 8.0) buffer. Antibody selection from the reaction mixture was performed with the originally described human To autoimmune reference serum (Reddy et al., 1983; kindly provided by Eng Tan, Scripps Research Institute, La Jolla, CA) prebound to protein A-Sepharose as previously described (Patton et al., 1989). RNA was extracted from the bound fraction after elution and analyzed by denaturing polyacrylamide gel electrophoresis. Other antibody selection experiments were done with a second autoimmune serum which contains antibodies against MRP RNA-containing ribonucleoprotein particles, human serum L122 (kindly provided by Walter van Venrooij, University of Nijmegen), or the murine monoclonal antibody 72B9 to human fibrillarin (Reimer et al., 1987; kindly provided by Michael Pollard and Eng Tan, Scripps Research Institute).

### Cell Culture, Microinjection, and Immunocytochemistry

A subclone of normal rat kidney epithelial cells (NRK-52E; Amer. Type Culture Collection, Rockville, MD) was cultured in F-12K medium (JRH Bioscience, Lenexa, KS) containing 10% FBS (JRH Bioscience, Lenexa, KS), 1 mM L-glutamine, 50  $\mu$ g/ml streptomycin, and 50  $\mu$ g/ml penicillin. Cells were plated onto glass coverslips and cultured at 37°C in 5% CO<sub>2</sub> for 36–48 h before experiments (McKenna and Wang, 1989). Nuclear microinjections were performed pneumatically as previously described (Wang et al., 1991). All the experiments were done with actively growing cells in subconfluent cultures. Microinjection did not cause cell damage as assessed by phase contrast microscopy. Cells were cultured in an incubation chamber with temperature and CO<sub>2</sub> regulation on the microscope stage during microinjection and the subsequent period of observation (McKenna and Wang, 1989).

For immunocytochemistry, cells were fixed with prewarmed (37°C) 4% formaldehyde in phosphate-buffered saline (PBS; pH 7.0) for 10 min at

37°C, rinsed twice with PBS and either imaged immediately or permeabilized with prechilled 0.8% Triton X-100 in PBS-containing 1% bovine serum albumin (BSA) for 5 min on ice, blocked with PBS-containing 1% BSA for 20 min at room temperature, and then incubated for 16 h at 4°C with either a murine monoclonal antibody to fibrillarin (72B9; Reimer et al., 1987) or the human autoimmune To reference serum (Reddy et al., 1983) in PBS-containing 1% BSA. After washing extensively with PBS-containing 1% BSA, the secondary antibody, either fluorescein-conjugated sheep anti-mouse IgG (Sigma Chem. Co.) or rhodamine-conjugated goat anti-human IgG (Pierce, Rockford, IL), was added and the coverslip was incubated for 2 h at 37°C. The cells were subsequently washed with PBS-containing 1% BSA (at room temperature for  $\sim$ 30 min with three changes of buffer) and examined by fluorescence microscopy.

### Fluorescent Microscopy and Image Processing

All observations were made with a Zeiss Axiovert-10 inverted fluorescence microscope equipped with a 100 $\times$ /NA 1.30 Neofluar Ph 3 objective, a 40X/NA 1.0 Apochromat objective, and a 40 $\times$ /NA 0.65 F/Apochromat Ph2 objective. A 12 V, 100-W quartz-halogen lamp was used as the light source for epi-illumination. Bandpass filters (Zeiss No. 487915 for rhodamine and No. 487917 for fluorescein) were used for fluorescence observations, and no crossover between fluorescein and rhodamine was detectable. Fluorescence images were acquired with a cooled-CCD camera (Star I; Photometrics, Tucson, AZ) linked to a Personal IRIS 4D/20 workstation (Silicon Graphics Inc., Mountain View, CA) and image processor (Series 150; Image Technology, Woburn, MA) for data storage and display. To preserve the geometry of the displayed image, the pixel aspect ratio of the CCD images was converted from 1:1 to 5:4 before input into the image processor which displays images as arrays of rectangular (5:4) pixels. Typical exposure times were 15 s for both living and fixed cells. To generate superimposed images, paired images were placed into registration by rapidly alternating the display between the two images, while moving one image relative to the other until no wobbling was observed (Cao and Wang, 1990; Cao et al., 1993). Hardcopies of images were generated using a Kodak ColorEase PS printer (Eastman Kodak Company, Rochester, NY). Digital optical sections were obtained using a computer-controlled stepping motor (0.25  $\mu$ m step size). Removal of out of focus light in optical slices was achieved using the nearest neighbor algorithm (Castleman, 1979; Agard, 1984; Shaw and Rawlings, 1991) and point spread functions obtained with our optical system, as previously described (Fishkind and Wang, 1993). Three-dimensional reconstruction of x-y stereo pairs were produced by stacking a set of deconvolved sections and projecting them angled at +10° and -10° from the optical axis (Fishkind and Wang, 1993).

## Results

### In Vitro Assembly of Fluorescently Labeled MRP RNA

Human MRP RNA (Fig. 1) readily associates with a  $\sim$ 40,000-mol wt protein, the To antigen (Yuan et al., 1991), which is present in HeLa cell extracts. The To antigen was initially identified using patient sera containing antibodies directed against MRP RNA-containing ribonucleoprotein particles (Reimer et al., 1988; Kipnis et al., 1990). As shown in Fig. 2 A, both rhodamine-coupled and noncoupled MRP RNA assembled into a ribonucleoprotein complex immunoselectable by To autoimmune serum. Fig. 2 B further shows, via direct immunoselection of the fluorescent MRP RNA itself, that it assembles into a ribonucleoprotein with the To antigen but does not associate with fibrillarin, as a negative control. These results establish that, at our level of rhodamine coupling (5–8 rhodamines per MRP RNA molecule), the fluorochrome labeling does not significantly impair the assembly of MRP RNA into the To ribonucleoprotein complex, nor does it induce MRP RNA to spuriously bind other proteins (e.g., fibrillarin).

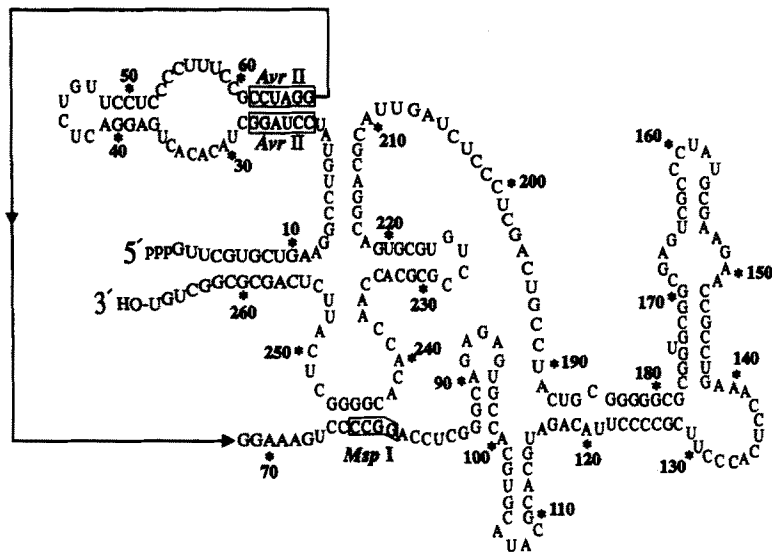


Figure 1. Human MRP RNA. The secondary structure is that proposed by Schmitt et al. (1993). The solid line represents a single phosphodiester bond linkage between nucleotides 67 and 68. The recognition sequences for AvrII and MspI are indicated.

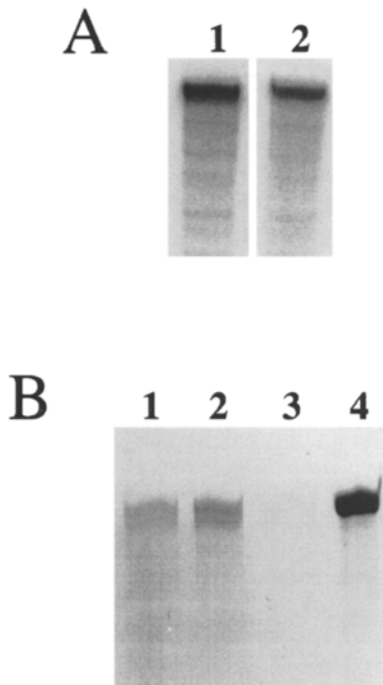


Figure 2. Reconstitution of MRP RNA with the To antigen. (A) Equal amounts of  $^{32}\text{P}$ -labeled MRP RNA (lane 1) or  $^{32}\text{P}$ - and rhodamine-labeled MRP RNA (lane 2) were purified, incubated with a HeLa cell extract, immunoselected with To reference serum (Reddy et al., 1983), and resolved by denaturing polyacrylamide gel electrophoresis as described in Materials and Methods. (B) Rhodamine-labeled MRP RNA was incubated with HeLa cell extract as in A and immunoselected with the original human To reference serum (lane 1), L122 serum (another MRP RNA-RNP monospecific patient serum, see Materials and Methods; lane 2), or monoclonal antibody 72B9 (anti-fibrillarlin; lane 3), and directly examined by fluorescence after denaturing polyacrylamide gel electrophoresis. Lane 4 is rhodamine-labeled MRP RNA as a reference. This is a reverse-contrast photograph of the fluorescence copy print (i.e., black, RNA fluorescence).

### Localization of Nucleus-microinjected RNase MRP RNA

To examine the movement and localization of the RNA component of RNase MRP in the nucleus, rhodamine-labeled MRP RNA was microinjected into the nuclei of normal rat kidney (NRK) cells (Fig. 3). At the earliest timepoint examined after nuclear microinjection (4 min, Fig. 3 b), most of the rhodamine-labeled MRP RNA was localized in nucleoli. We have consistently observed this strikingly rapid nucleolar localization of MRP RNA. Over time, the amount of nucleolus-localized MRP RNA decreased and signal subsequently appeared in both the nucleoplasm and cytoplasm (Fig. 3, b-f). The numerous cytoplasmic foci observed 3 h after nuclear microinjection (Fig. 3, d and f) were highly motile as visualized by time-lapse fluorescence imaging (data not shown). Although we have not further identified these cytoplasmic sites, MRP RNA has been localized in mitochondria by ultrastructural in situ hybridization (Li et al., 1994).

The cell microinjected in Fig. 3 is binucleate. It can be seen that, once in the cytoplasm, the rhodamine-labeled MRP RNA did not enter the other nucleus of this cell (see Fig. 3, d and f), indicating that MRP RNA lacks signals for cytoplasm to nucleus traffic. When rhodamine-labeled MRP RNA was microinjected into the cytoplasm of NRK cells (Fig. 4), we similarly observed the accumulation of signal in numerous cytoplasmic spots which were highly motile (not shown). As can be seen, cytoplasm-microinjected MRP RNA did not enter the nucleus, even after longer incubation times (Fig. 4 b).

The rapidity with which MRP RNA become localized in nucleoli (Fig. 3 b) is striking. To examine even earlier timepoints, cells were fixed with 4% formaldehyde immediately after nuclear microinjection. As shown in Fig. 5, a-e, MRP RNA was predominantly localized in nucleoli as early as 30 s after nuclear microinjection. This extremely fast nucleolar localization of MRP RNA contrasts with our previously described, more gradual movement of microinjected pre-mRNAs to nucleoplasmic sites of accumulation, which takes ~30-60 min (Wang et al., 1991).

Fig. 5 f shows that MRP RNA injected into the cyto-

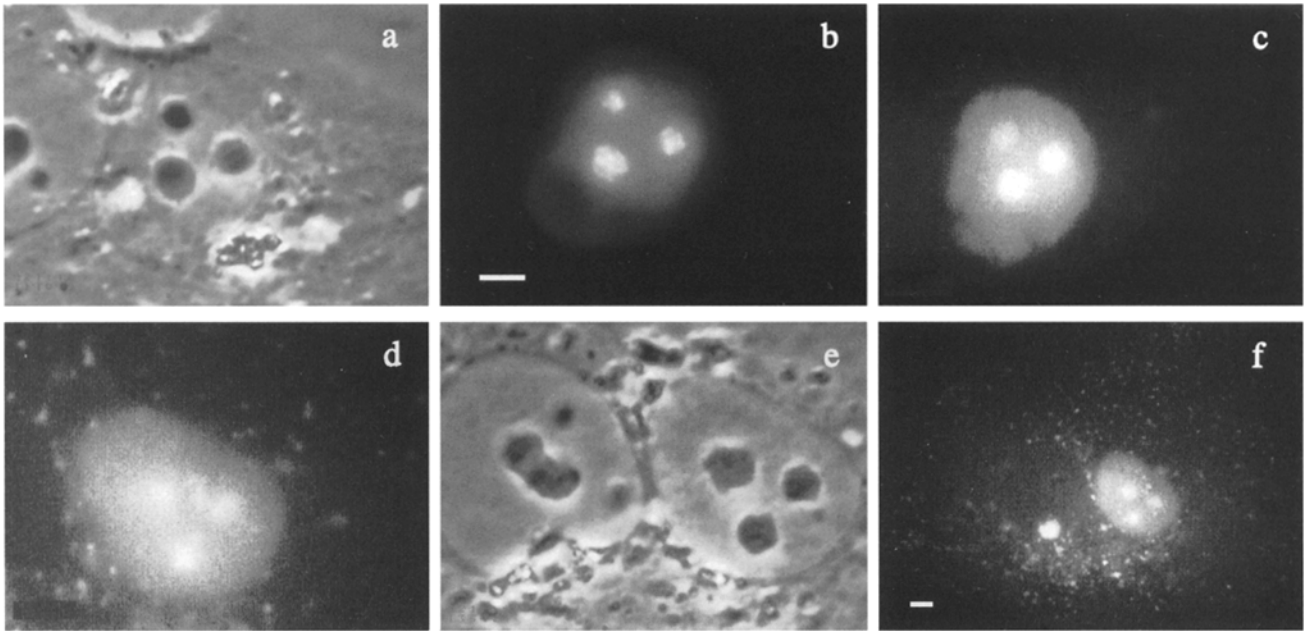


**Figure 3.** Localization of human RNase MRP RNA after microinjection into the nucleus of NRK cells. MRP RNA was transcribed *in vitro*, labeled with rhodamine, purified and microinjected into the nucleus of NRK cells as described in Materials and Methods. The subsequent localization of MRP RNA was visualized in the same living cell at 4 min (*b*), 25 min (*c*), and 3 h (*d* and *f*). Phase contrast images of the cell at 4 min and 3 h after nuclear microinjection are shown in *a* and *e*, respectively. Note that this cell is binucleate (see Results), and that the nuclei have reoriented during the course of observation. We have seen such reorientation in numerous other experiments when the observation period extends to 1–3 h. Bar: (*b* and *e*) 5  $\mu\text{m}$ .

plasm is, after 5 min, diffusely distributed. This early, non-localized cytoplasmic distribution is of interest in relation to the punctate cytoplasmic foci seen at later times after cytoplasmic injection (Fig. 4).

#### **Digital Optical Sectioning Microscopy and 3-D Analysis of Nucleolar Localized MRP RNA**

Using fluorescence microscopy in combination with digital optical sectioning microscopy, we sought to determine whether the localization of nucleus-microinjected MRP RNA actually occurs throughout the nucleolus or perhaps

only on the nucleolar surface. A through-focus series of optical sections (0.25  $\mu\text{m}$  step size) for the same cell observed in Fig. 5 *c* was obtained (Fig. 6, panel *A*) and out of focus light was removed by digital image processing (Fig. 6, panel *B*) as described in Materials and Methods. Analysis of the optical sections through the cell nucleus in Fig. 6 (panels *A* and *B*), as well as the three-dimensional stereo pairs generated from these optical sections (panel *C*), demonstrated that the localized MRP RNA was present throughout the nucleoli in an interlinking network of lobular foci connected by thinner strands, which is the classical organization of the dense fibrillar component as defined

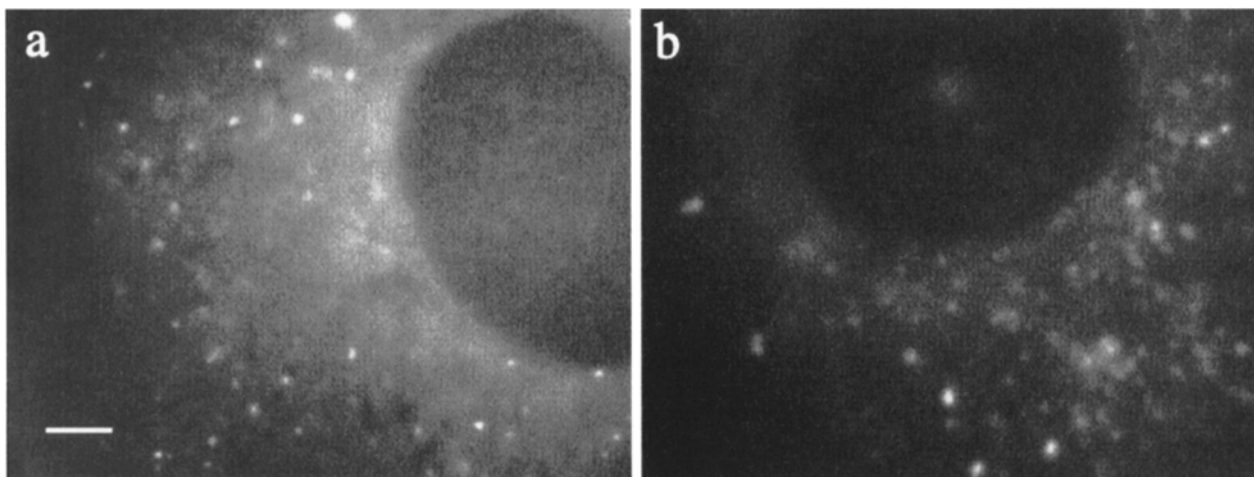


**Figure 4.** Localization of MRP RNA after microinjection into the cytoplasm. Rhodamine-labeled MRP RNA was microinjected into the cytoplasm of NRK cells and visualized 16 min (*a*) or 73 min (*b*) after microinjection. Bar, 5  $\mu\text{m}$ .

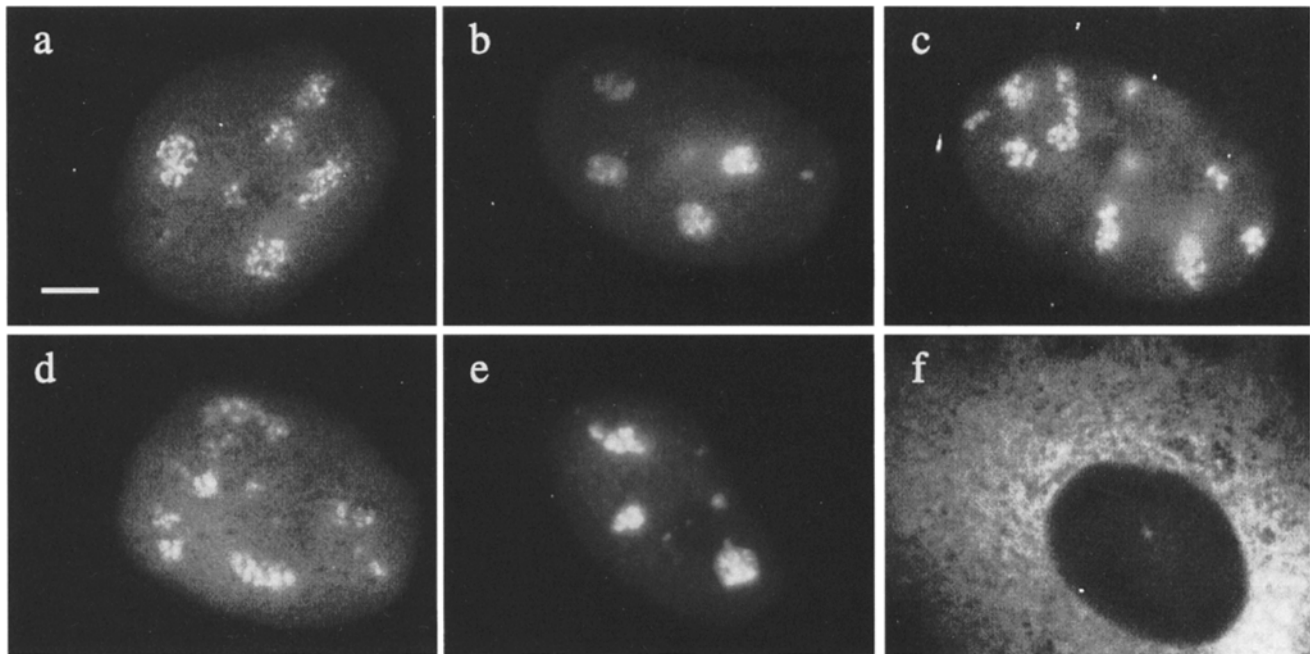


**Figure 5.** Rapid localization of MRP RNA in subnucleolar structures after nuclear microinjection. NRK cells were nucleus-microinjected with either rhodamine-labeled (*a*, *b*, *d*, and *e*) or fluorescein-labeled (*c*) MRP RNA or cytoplasm-microinjected with rhodamine-labeled MRP RNA (*f*), fixed 30 s (*a*), 1 min (*b*), 3 min (*c* and *d*), and 5 min (*e* and *f*) after microinjection and visualized by fluorescence microscopy as described in Materials and Methods. Bar, 5  $\mu$ m.

by electron microscopy (Fakan and Bernhard, 1971; Hadjiolov, 1985; Thiry and Thiry-Blaise, 1989; Puvion-Dutilleul et al., 1991; Thiry and Thiry-Blaise, 1991).

#### **Microinjected MRP RNA Localizes to the Dense Fibrillar Component of the Nucleolus**

To determine if the nucleolar sites of MRP RNA localization indeed correspond to the dense fibrillar component, cells were nucleus-microinjected with rhodamine-labeled MRP RNA, fixed within 1 min after microinjection, and the spatial localization of MRP RNA within the nucleolus was compared with that of fibrillarin, a dense fibrillar component protein (Ochs et al., 1985; Reimer et al., 1987; Scheer and Benavente, 1990) associated with several small nucleolar ribonucleoprotein particles involved in pre-rRNA processing (Tyc and Steitz, 1989). As shown in Fig. 7, rhodamine-labeled MRP RNA (Fig. 7 *a*; *red*) and fibrillarin (Fig. 7 *b*; *green*) displayed virtually identical patterns in the nucleoli. Superimposition of these two images revealed a very precise colocalization, as indicated by the yellow signal in Fig. 7 *c*.

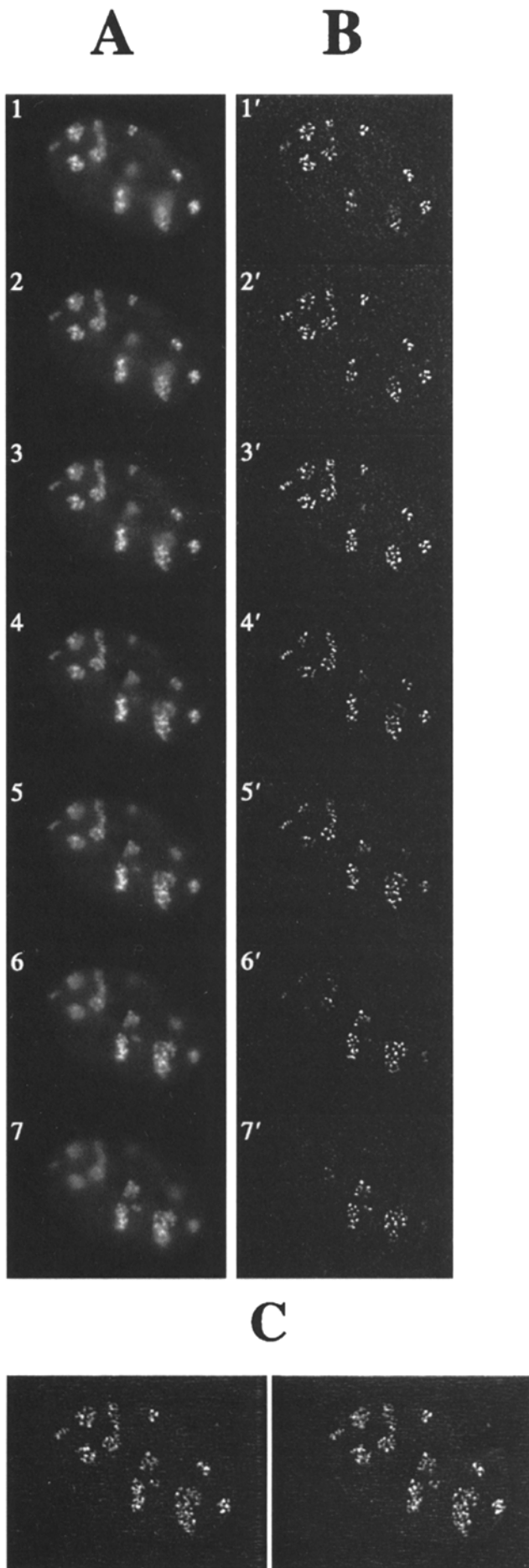
#### **The To Antigen-binding Domain of MRP RNA Is Necessary for Nucleolar Localization**

Sera from certain autoimmune disease patients contain antibodies which recognize a  $\sim$ 40,000-mol wt nuclear protein, the To antigen (Reimer et al., 1988; Kipnis et al., 1990). To antisera also immunoselect a MRP RNA-containing RNP complex (Reddy et al., 1983; Reimer et al., 1988). As can be seen in Fig. 8, the antigenic protein recognized by the original To reference serum (Reddy et al., 1983) is localized predominantly in the nucleolus, with an

indication of particular concentration in an array of subnucleolar elements that resemble the dense fibrillar component.

The To antigen binds nucleotides 21-64 of human MRP RNA (Yuan et al., 1991). We therefore examined the importance of this To antigen-binding site in the observed rapid nucleolar localization of nucleus-microinjected MRP RNA. Clones encoding human MRP RNAs were constructed in which nucleotides 23-62 of MRP RNA were deleted or replaced. As shown in Fig. 9 *d*, deletion of the To-binding site of MRP RNA resulted in a diffuse nucleoplasmic distribution at early times after nuclear microinjection, with no sign of nucleolar localization. Similarly, nuclear microinjection of a mutant MRP RNA in which the To-binding site was altered within the loop regions also resulted in a diffuse pattern throughout the nucleoplasm after microinjection, with no nucleolar localization (Fig. 9 *f*). Even at later times after microinjection, no nucleolar localization was observed with either of the mutant MRP RNAs (data not shown) pointing to the importance of the To antigen-binding domain.

To determine if other regions of MRP RNA are also necessary for nucleolar localization, we injected into the nucleus a shortened MRP RNA containing only nucleotides 1-79. As shown in Fig. 10, this RNA also became localized in nucleoli. However, the shortened MRP RNA disappeared from the cell altogether within 10-15 min after microinjection (data not shown). While this observation may reflect the dispersion of the 1-79 nucleotide RNA to sites of lower concentration (below the light detection limit of our microscopy system), the initial nucleolar localization of this RNA (Fig. 10) suggests that sequences within nucleotides 1-79 of MRP RNA are sufficient for nucleolar localization.



## Discussion

The methods we have developed (Wang et al., 1991, and this paper) for visualizing RNA molecules introduced into living cells can be thought of both as having a "staining" aspect, i.e., affinity of the introduced RNA for immobile intranuclear sites (hence the use of the classical term cytochemistry), but also potentially as a tracer approach for observing dynamic pathways of RNA traffic. We have typically introduced 5,000–10,000 molecules of RNA, each carrying ~5–8 rhodamine groups. The fluorescence signal intensity resulting from a single RNA molecule (between 100–400 nucleotides long) is below the sensitivity of our detection system. When a large proportion of the introduced RNAs accumulate at a relatively small number of intracellular sites, the resulting fluorescent signals are readily detected.

RNase MRP was initially identified as an activity that, *in vitro*, cleaves mitochondrial transcripts into molecules that can serve as primers for mitochondrial DNA replication (Chang and Clayton, 1987a). When RNase MRP was discovered to be a ribonucleoprotein enzyme and its essential RNA (MRP RNA) component was sequenced (Chang and Clayton, 1987b), it turned out to be identical to a previously defined nucleolar RNA, termed 7-2 RNA (Gold et al., 1989; Yuan et al., 1989). MRP RNA has been detected in mitochondria by *in situ* hybridization (Li et al., 1994), but the great majority of MRP RNA (7-2 RNA) in the cell fractionates with nucleoli (Reddy et al., 1981). Our demonstration that MRP RNA microinjected into the nucleus rapidly accumulates in nucleoli is entirely consistent with the original localization of MRP RNA (7-2 RNA) as determined by nuclear fractionation.

We have also shown that MRP RNA rapidly accumulates in the dense fibrillar component (DFC) of the nucleolus after nuclear microinjection. As facilitated by fluorescence microscopy, digital optical sectioning, and 3-D stereo visualization (Fig. 6), our images of fluorescent MRP RNA display the DFC at a higher resolution than has been previously achieved in the light microscope. In addition, we have recently carried out *in situ* hybridization experiments in nontransformed human fibroblasts and in NRK cells and find that the endogenous MRP RNAs in these cell lines are also concentrated in the DFC (Jacobson, M. R., K. Taneja, R. H. Singer, and T. Pederson, unpublished results). Thus, there is also a strong concordance of our fluorescent RNA results with the *in situ* localization of endogenous nuclear MRP RNA. This local-

**Figure 6.** Digital optical sectioning microscopy and 3-D reconstruction of nucleolar localized MRP RNA. A through-focus series of optical sections (0.25  $\mu\text{m}$  step size) was obtained of a cell nucleus microinjected with fluorescein-labeled MRP RNA (the same cell observed in Fig. 5 c) as described in Materials and Methods. (A) Serial sequence of optical sections showing the "raw" fluorescence images. (B) The corresponding deconvolved optical sections showing increased apparent resolution and contrast of structures after removal of out of focus light and contrast enhancement. (C) A 3-D stereo pair produced by stacking the set of deconvolved sections and projecting the images angled at  $+10^\circ$  and  $-10^\circ$  from the optical axis, as described in Materials and Methods. The optical sections are numbered directionally from bottom to top.

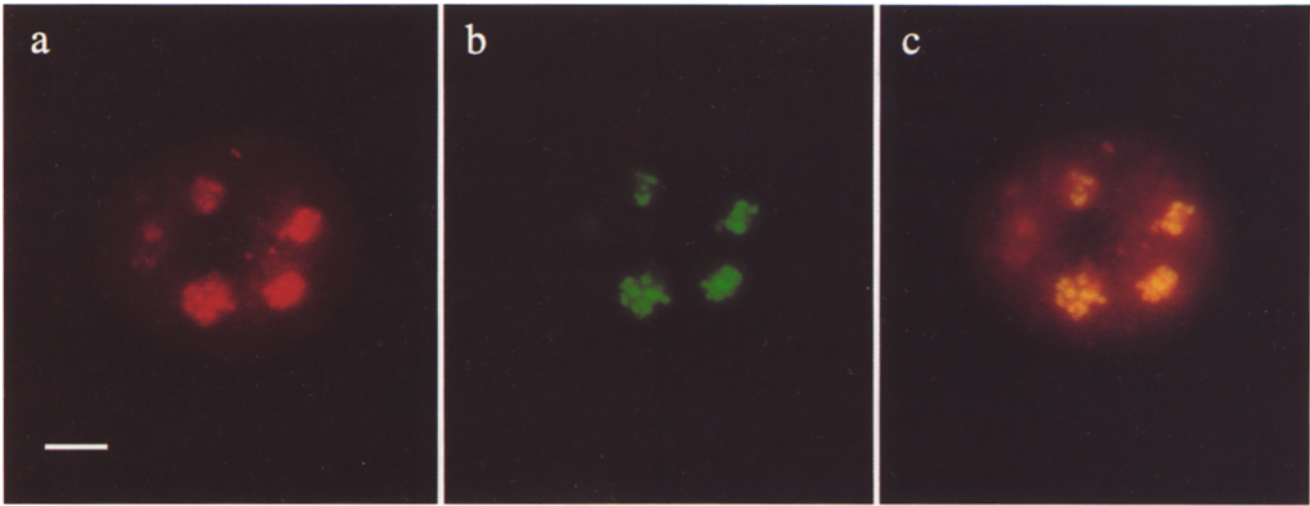


**Figure 7.** MRP RNA rapidly localizes in the dense fibrillar component of the nucleolus after nuclear microinjection. NRK cells were nucleus-microinjected with rhodamine-labeled MRP RNA, fixed  $\sim 1$  min after microinjection, permeabilized and stained for fibrillarin as described in Materials and Methods. Antibody-antigen complexes were detected with fluorescein-conjugated anti-mouse IgG. (a) Rhodamine-labeled MRP RNA (*red*); (b) endogenous fibrillar fibrillarin (*green*); (c) superimposition of a and b. Bar, 5  $\mu\text{m}$ .

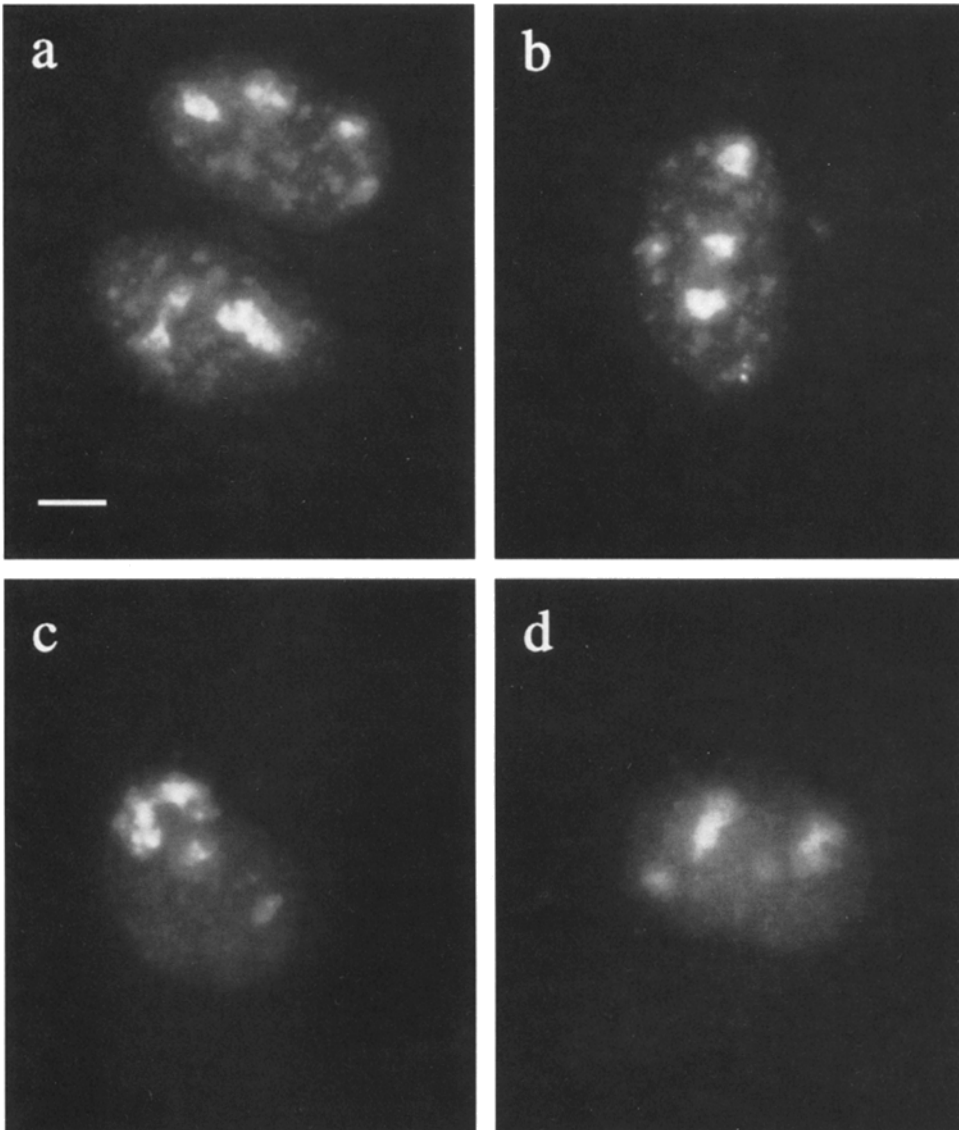


**Figure 8.** Immunocytochemical localization of the To antigen. NRK cells were fixed, permeabilized, and stained for the To antigen using the original To reference serum (Reddy et al., 1983) as described in Materials and Methods. Antibody-antigen complexes were detected with rhodamine-conjugated anti-human IgG. (a-d) Four representative examples. Bar, 5  $\mu\text{m}$ .

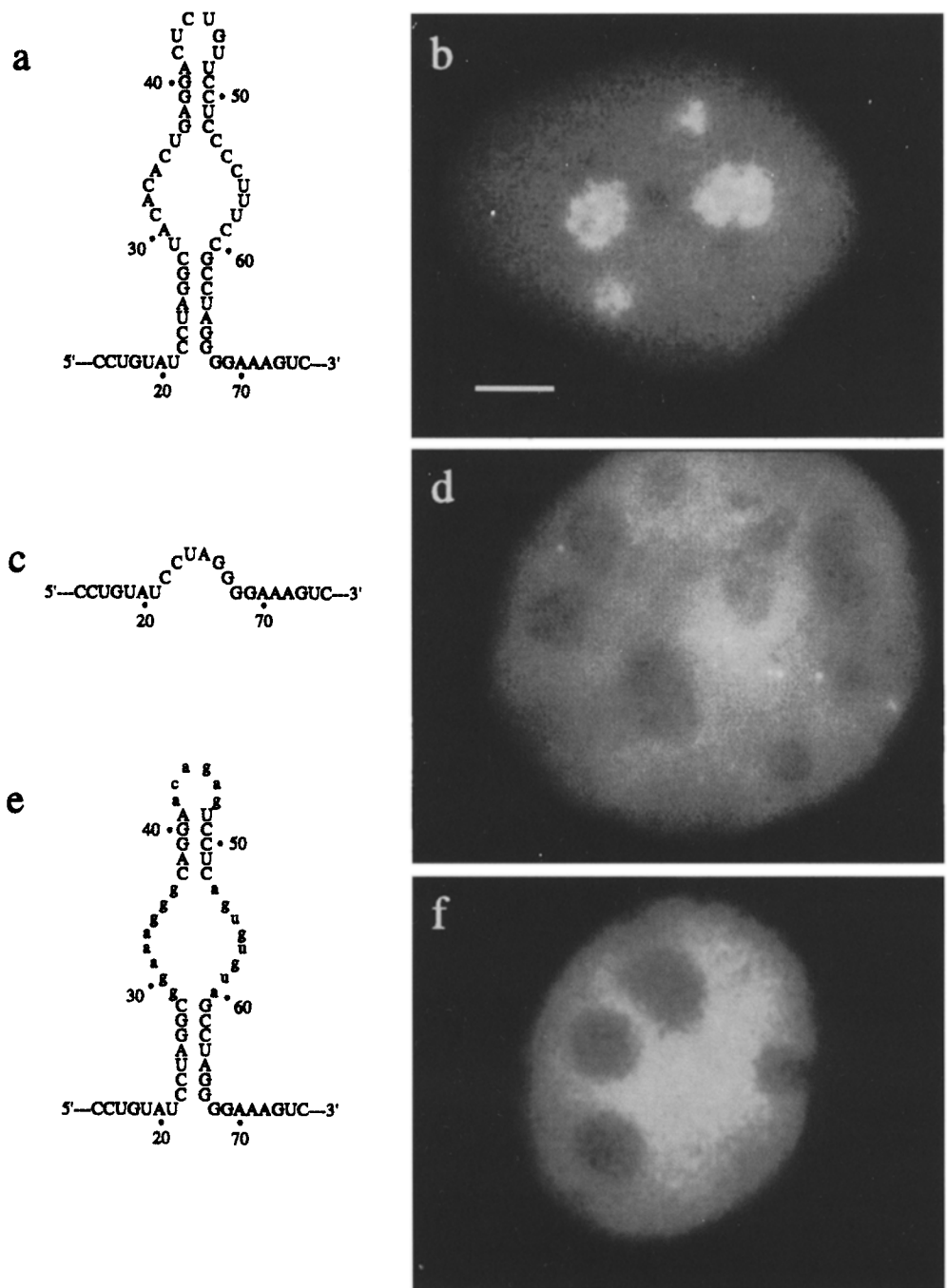


**Figure 9.** Nucleolar localization of MRP RNA requires the To antigen-binding site. The sequence and secondary structure of the region encompassing the To antigen-binding domain (nucleotides 21–64; Yuan et al., 1991) of wild-type human MRP RNA (a) and mutants MRP-1 (c) and MRP-2 (e) RNAs are indicated. (b) Rhodamine-labeled MRP RNA (wild-type MRP RNA) was visualized in a living cell 5 min after nuclear microinjection. (d) Rhodamine-labeled MRP-1 RNA was visualized in a living cell 2 min after nuclear microinjection. (f) Rhodamine-labeled MRP-2 RNA was visualized in a living cell 4 min after nuclear microinjection. Bar, 5  $\mu$ m.

ization of MRP RNA in the DFC likely relates to its role in pre-rRNA processing, specifically in the 5'-end cleavage of the 5.8 S–25 S rRNA intermediate (Schmitt and Clayton 1993; Chu et al., 1994; Lygerou et al., 1994).

A recent fluorescence in situ hybridization study reported that in HeLa cells, a human transformed line, MRP RNA was localized in nucleoli, especially in perinucleolar foci (Matera et al., 1995). We have seen no evidence of such perinucleolar sites of MRP RNA concentration in either our fluorescent RNA cytochemistry work or in situ hybridization experiments, all carried out with nontransformed cells (see also Discussion in Matera et al., 1995). Our results are consistent with the previous nucleolar localization of the To antigen by immunoelectron micros-

copy (Reimer et al., 1988); we note that the micrographs in this paper revealed most of the gold particles to be located at or near junctions of the granular component with the DFC (see Figs. 3 and 4 in Reimer et al., 1988). As we report here, much of the nucleolar To antigen appears to also be concentrated in a pattern that strongly resembles the DFC as visualized by high resolution fluorescence microscopy (Fig. 8).

Analysis of microinjected mutant RNAs demonstrates that the To antigen-binding domain is necessary for nucleolar localization of MRP RNA. These data suggest that either nucleoplasmic To antigen (see Fig. 8) binds and directly targets MRP RNA to the nucleolus or that nucleolar localized To antigen is a high affinity site for MRP RNA



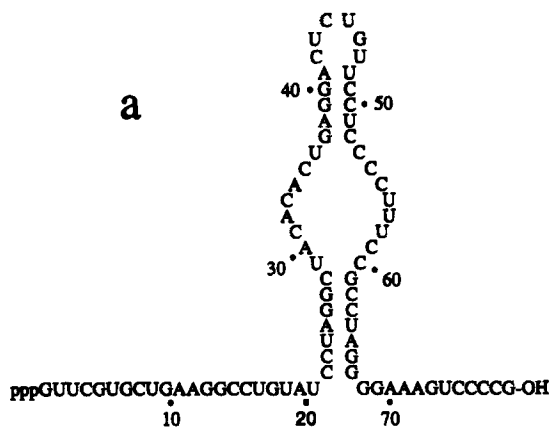
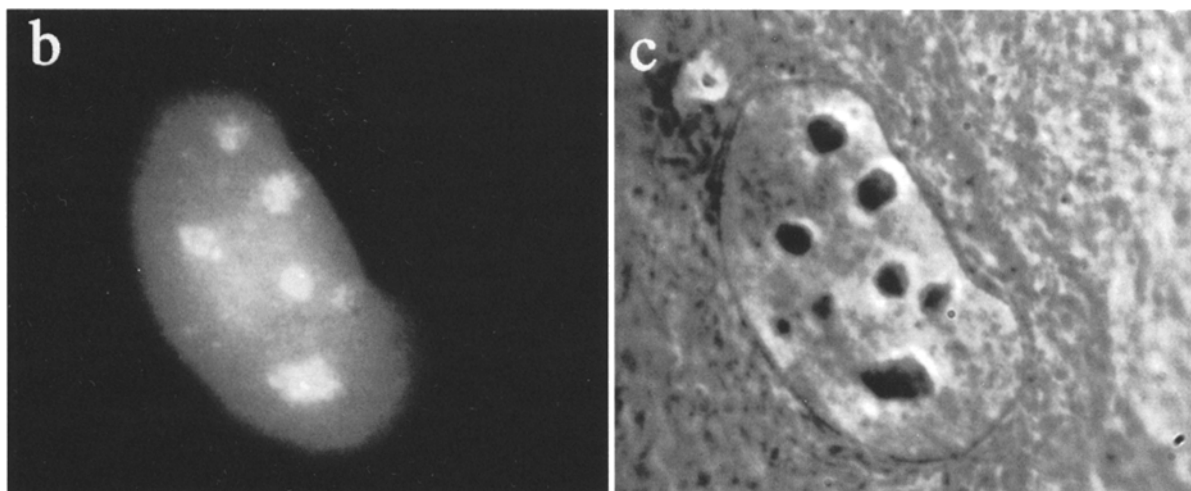


**Figure 10.** Rapid nucleolar localization of a “mini-MRP RNA” (nucleotides 1–79) containing the To antigen-binding domain. The mini-MRP RNA was transcribed from plasmid pHMRP<sub>MODT3</sub> after digestion with MspI, using T3 RNA polymerase in the presence of 5-(3-aminoallyl)UTP, coupled with rhodamine, purified, and microinjected into the nucleus of NRK cells all as described in Materials and Methods. (a) Sequence and proposed structure of the mini-MRP RNA (nucleotides 1–79). (b) Localization of rhodamine-labeled mini-MRP RNA visualized in a living cell 3 min after nuclear microinjection. (c) Phase image of the cell in b.



accumulation. Although the protein components of enzymatic RNase MRP remain unknown, and as such their role in the nucleolar accumulation of MRP RNA cannot be assessed, rapid nucleolar localization of the “mini-MRP” RNA (nucleotides 1–79) suggests the To antigen-binding domain may be sufficient for nucleolar localization. The site of RNase MRP assembly is also unknown. However, the rapidity with which wild-type MRP RNA (and the mini-MRP RNA) localized in the nucleolar DFC is consistent with it being the site of RNase MRP assembly as well as a site of catalytic activity. Further studies are necessary to more fully elucidate this important point.

How various RNAs that are generated in the nucleoplasm are targeted for the nucleolus is a major unsolved problem in the cell biology of the nucleus. For example, 5 S rRNA is transcribed on nucleoplasmic genes and yet associates with the nucleolus (Long and Dawid, 1980). In addition, many newly discovered small nucleolar RNAs (snoRNAs) originate in the introns of nucleoplasmic genes (for a recent review see Maxwell and Fournier, 1995). These traffic patterns are not well understood (although see Steitz et al., 1988). This exciting new aspect of RNA processing and intranuclear traffic awaits identification of the nucleolar targeting signals involved. Our fluorescent RNA cytochemistry method in combination with the molecular mutagenesis of cloned RNAs offers promise for the identification of various RNA domains responsible for

nucleolar targeting, as well as for other traffic and localization pathways in the cell.

We thank Tamás Kiss and Witold Filipowicz (Friedrich Miescher-Institut) for plasmid pHMRP<sub>MODT3</sub>; Michael Pollard and Eng Tan (Scripps Research Institute) for monoclonal antibody 72B9; Eng Tan (Scripps Research Institute) for the human To reference serum (No. A2106); and Helma Pluk and Walter van Venrooij (University of Nijmegen) for the MRP RNA-RNP monospecific human serum L122. We also thank Roxanne Labrecque for her excellent technical support in this project. We are grateful to Joel Richter and David Wolf (Worcester Foundation) for critically reading the manuscript.

This work was supported by grants from the National Institutes of Health to T. Pederson (GM-21595-21) and to Y.-L. Wang (GM-32476-10).

Received for publication 21 March 1995 and in revised form 27 September 1995.

#### References

- Agard, D. A. 1984. Optical sectioning microscopy: cellular architecture in three dimensions. *Annu. Rev. Biophys. Bioeng.* 13:191–219.
- Agrawal, S., C. Christodoulou, and M. J. Gait. 1986. Efficient methods for attaching non-radioactive labels to the 5' ends of synthetic oligodeoxyribonucleotides. *Nucleic Acids Res.* 14:6227–6245.
- Cao, L.-G., and Y.-L. Wang. 1990. Mechanism of the formation of contractile ring in dividing cultured animal cells. I. Recruitment of preexisting actin filaments into the cleavage furrow. *J. Cell Biol.* 110:1089–1095.
- Cao, L.-G., D. J. Fishkind, and Y.-L. Wang. 1993. Localization and dynamics of nonfilamentous actin in cultured cells. *J. Cell Biol.* 123:173–181.
- Castleman, K. R. 1979. *Digital Image Processing*. Prentice-Hall, Englewood Cliffs, NJ. 429 pp.
- Chang, D. D., and D. A. Clayton. 1987a. A novel endoribonuclease cleaves at a

- priming site of mouse mitochondrial DNA replication. *EMBO (Eur. Mol. Biol. Organ.) J.* 6:409-417.
- Chang, D. D., and D. A. Clayton. 1987b. A mammalian mitochondrial RNA processing activity contains nucleus-encoded RNA. *Science (Wash. DC)*. 235:1178-1184.
- Chang, D. D., and D. A. Clayton. 1989. Mouse RNase MRP RNA is encoded by a nuclear gene and contains a decamer sequence complementary to a conserved region of mitochondrial RNA substrate. *Cell*. 56:131-139.
- Chu, S., R. H. Archer, J. M. Zegel, and L. Lindahl. 1994. The RNA of RNase MRP is required for normal processing of ribosomal RNA. *Proc. Natl. Acad. Sci. USA*. 91:659-663.
- Fakan, S., and W. Bernhard. 1971. Localization of rapidly and slowly labeled nuclear RNA as visualized by high resolution autoradiography. *Exp. Cell Res.* 67:129-141.
- Fishkind, D. J., and Y.-L. Wang. 1993. Orientation and three-dimensional organization of actin filaments in dividing cultured cells. *J. Cell Biol.* 123:837-848.
- Gold, H. A., J. N. Topper, D. A. Clayton, and J. Craft. 1989. The RNA processing enzyme RNase MRP is identical to the Th RNP and related to RNase P. *Science (Wash. DC)*. 245:1377-1380.
- Hadjiolov, A. A. 1985. *The Nucleolus and Ribosome Biogenesis*. Springer-Verlag, New York. 268 pp.
- Hashimoto, C., and J. A. Steitz. 1983. Sequential association of nucleolar 7-2 RNA with two different autoantigens. *J. Biol. Chem.* 258:1379-1382.
- Kipnis, R. J., J. Craft, and J. A. Hardin. 1990. The analysis of antinuclear and antinucleolar autoantibodies of scleroderma by radioimmunoprecipitation assays. *Arthritis Rheum.* 33:1431-1437.
- Kiss, T., C. Marshallsay, and W. Filipowicz. 1992. 7-2/MRP RNAs in plant and mammalian cells: association with higher order structures in the nucleolus. *EMBO (Eur. Mol. Biol. Organ.) J.* 11:3737-3746.
- Langer, P. R., A. A. Waldrop, and D. C. Ward. 1981. Enzymatic synthesis of biotin-labeled pony nucleotides: novel nucleic acid affinity probes. *Proc. Natl. Acad. Sci. USA*. 78:6633-6637.
- Li, K., C. S. Smagula, W. J. Richardson, M. Gonzalez, H. K. Hagler, and R. S. Williams. 1994. Subcellular partitioning of MRP RNA assessed by ultrastructural and biochemical analysis. *J. Cell Biol.* 124:871-882.
- Long, E. O., and I. B. Dawid. 1980. Repeated genes in eukaryotes. *Annu. Rev. Biochem.* 49:727-764.
- Lygerou, Z., P. Mitchell, E. Petfalski, B. Séraphin, and D. Tollervey. 1994. The POP1 gene encodes a protein component common to the RNase MRP and RNase P ribonucleoproteins. *Genes & Dev.* 8:1423-1433.
- Matera, A. G., M. R. Frey, K. Margelot, and S. L. Wolin. 1995. A perinucleolar compartment contains several RNA polymerase III transcripts as well as the polypyrimidine tract-binding protein, hnRNP I. *J. Cell Biol.* 129:1181-1193.
- Maxwell, E. S., and M. J. Fournier. 1995. The small nucleolar RNAs. *Annu. Rev. Biochem.* 35:897-934.
- McKenna, N. M., and Y.-L. Wang. 1989. Culturing cells on the microscope stage. *Methods Cell Biol.* 29:195-205.
- Ochs, R. L., M. A. Lischwe, W. H. Spohn, and H. Busch. 1985. Fibrillarlin: a new protein of the nucleolus identified by autoimmune sera. *Biol. Cell*. 54:123-134.
- Patton, J. R., R. J. Patterson, and T. Pederson. 1987. Reconstitution of the U1 small nuclear ribonucleoprotein particle. *Mol. Cell. Biol.* 7:4030-4037.
- Patton, J. R., W. Habets, W. J. van Venrooij, and T. Pederson. 1989. U1 small nuclear ribonucleoprotein particle-specific proteins interact with the first and second stem-loops of U1 RNA, with the A protein binding directly to the RNA independently of the 70K and Sm proteins. *Mol. Cell. Biol.* 9:3360-3368.
- Puvion-Dutilleul, F., J. P. Bachellerie, and E. Puvion. 1991. Nucleolar organization of HeLa cells as studied by in situ hybridization. *Chromosoma*. 100:395-409.
- Reddy, R., W.-Y. Li, D. Henning, Y. C. Choi, K. Nohaga, and H. Busch. 1981. Characterization and subcellular localization of 7-8 S RNAs of Novikoff hepatoma. *J. Biol. Chem.* 256:8452-8457.
- Reddy, R., E. M. Tan, D. Henning, K. Nohaga, and H. Busch. 1983. Detection of a nucleolar 7-2 ribonucleoprotein and a cytoplasmic 8-2 ribonucleoprotein with autoantibodies from patients with scleroderma. *J. Biol. Chem.* 258:1383-1386.
- Reimer, G., K. M. Pollard, C. A. Penning, R. L. Ochs, M. A. Lischwe, H. Busch, and E. M. Tan. 1987. Monoclonal autoantibody from a (New Zealand black x New Zealand white) F1 mouse and some human scleroderma sera target and M<sub>r</sub> 34,000 nucleolar protein of the U3 RNP particle. *Arthritis Rheum.* 30:793-800.
- Reimer, G., I. Raska, U. Scheer, and E. M. Tan. 1988. Immunolocalization of 7-2 ribonucleoprotein in the granular component of the nucleolus. *Exp. Cell Res.* 173:117-128.
- Scheer, U., and R. Benavente. 1990. Functional and dynamic aspects of the mammalian nucleolus. *BioEssays*. 12:14-21.
- Schmitt, M. E., and D. A. Clayton. 1993. Nuclear RNase MRP is required for correct processing of pre-5.8S rRNA in *Saccharomyces cerevisiae*. *Mol. Cell. Biol.* 13:7935-7941.
- Schmitt, M. E., J. L. Bennett, D. J. Dairaghi, and D. A. Clayton. 1993. Secondary structure of RNase MRP RNA as predicted by phylogenetic comparison. *FASEB (Fed. Am. Soc. Exp. Biol.) J.* 7:208-213.
- Shaw, P. J., and D. J. Rawlings. 1991. Three-dimensional fluorescence microscopy. *Prog. Biophys. Mol. Biol.* 56:187-213.
- Steitz, J. A., C. Berg, J. P. Hendrick, H. La Branche-Chabot, A. Metzpalu, J. Rinke, and T. Yario. 1988. A 5S rRNA/L5 complex is a precursor to ribosome assembly in mammalian cells. *J. Cell Biol.* 106:545-556.
- Thiry, M., and L. Thiry-Blaise. 1989. In situ hybridization at the electron microscopy level: an improved method for precise localization of ribosomal DNA and RNA. *Eur. J. Cell Biol.* 50:235-243.
- Thiry, M., and L. Thiry-Blaise. 1991. Locating transcribed and non-transcribed rDNA spacer sequences within the nucleolus by in situ hybridization and immunoelectron microscopy. *Nucleic Acids Res.* 19:11-15.
- Topper, J. N., and D. A. Clayton. 1990. Characterization of human MRP/Th RNA and its nuclear gene: full length MRP/Th RNA is an active endoribonuclease when assembled as an RNP. *Nucleic Acids Res.* 18:793-799.
- Tyc, K., and J. A. Steitz. 1989. U3, U8 and U13 comprise a new class of mammalian snRNPs localized in the cell nucleolus. *EMBO (Eur. Mol. Biol. Organ.) J.* 8:3113-3119.
- Wang, J., L.-G. Cao, Y.-L. Wang, and T. Pederson. 1991. Localization of pre-messenger RNA at discrete nuclear sites. *Proc. Natl. Acad. Sci. USA*. 88:7391-7395.
- Yuan, Y., R. Singh, and R. Reddy. 1989. Rat nucleolar 7-2 RNA is homologous to mouse mitochondrial RNase mitochondrial RNA-processing RNA. *J. Biol. Chem.* 264:14835-14839.
- Yuan, Y., E. Tan, and R. Reddy. 1991. The 40-kilodalton To autoantigen associates with nucleotides 21 to 64 of human mitochondrial RNA processing/7-2 RNA in vitro. *Mol. Cell. Biol.* 11:5266-5274.